

The Effect of Iron Addition on the Dry Sliding Wear and Corrosion Behavior of Cu Al Ni Shape Memory Alloy

Dr. Abdul Raheem . K. Abid Ali * & Zuheir T. Khulief.Al-Tai *

Received on: 22/4/2010

Accepted on: 2/12/2010

Abstract

In this paper, dry sliding wear and corrosion behavior of Cu + 13wt% Al + 3.8 wt% Ni was prepared by powder metallurgy. Dry sliding wear has been studied based on pin on disk at constant velocity and constant sliding distance .Corrosion behavior in 5 wt% NaOH solution based up on potentiostatic (Tafel) has been presented for base shape memory alloy (Cu + 13% Al + 3.8 % Ni) in two cases austenitic and martensitic phase state . Further more , the effect of Fe additions as (0.4 , 0.8 and 1.2 wt%) on the sliding wear and corrosion behavior of base alloy has also been studied .It is clear that Cu Al Ni shape memory alloy in martensitic state has more wear resistance than in austenitic structure . Also , corrosion resistances are better than in martensitic structure because the alloy has corrosion current density as $336.45 \mu\text{A}/\text{cm}^2$ in martensitic where as the corrosion current density is $633.62 \mu\text{A}/\text{cm}^2$ in austenitic structure . Further more , when the iron content increases , wear and corrosion rate increase too .

Keywords : Shape memory alloys, Powder metallurgy, Cu Al Ni, Dry sliding, Corrosion behavior.

تأثير إضافة الحديد في البلى الانزلاقي الجاف وسلوك التآكل لسبيكة (نحاس
المنيوم نيكل) التي تتذكر شكلها.

الخلاصة:

في هذا البحث تم دراسة البلى الانزلاقي الجاف وسلوك التآكل للسبيكة (نحاس + 13% منيوم + 3.8% نيكل) المحضرة بطريقة ميتالورجيا المساحيق. البلى الانزلاقي الجاف درس باستخدام الترتيب المسماري إلى القرص تحت سرعة ثابتة ومسافة انزلاق ثابتة , السلوك التآكلي في محلول (5% هيدروكسيد الصوديوم) كنسبة وزنيه تم دراسته للسبيكة باستخدام طريقة استكمال منحنى تافل , حيث تم تحضير السبيكة الأساس (نحاس + 13% منيوم + 3.8% نيكل) في حالتين الأولى السبيكة في طور الاوستنايت والثانية في طور المارتنايت .بالإضافة إلى ذلك تم دراسة تأثير إضافة الحديد وبنسب (0.4 , 0.8 , 1.2) كنسب وزنيه في سلوك البلى الانزلاقي الجاف وسلوك التآكل . أظهرت النتائج إن سبيكة (نحاس - المنيوم - نيكل) في طور المارتنايت أكثر مقاومة للبلى مقارنة بالسبيكة في طور الاوستنايت , كذلك مقاومة التآكل أفضل للسبيكة في طور المارتنايت والتي امتلكت كثافة تيار تآكل بمقدار (336.45) مايكروامبيراسم² في حين للسبيكة في طور الاوستنايت (633.62 مايكروامبيراسم²). بالإضافة إلى ذلك عند زيادة محتوى الحديد فان معدل البلى والتآكل يزداد أيضا .

Introduction

During the past years, smart materials and structures have received increasing attention because of their great scientific and technological significance⁽¹⁾. Shape memory alloys are the most important branch from the smart and/or intelligence materials. The term "Shape memory alloys" refers to that group of metallic materials have the ability to return to some previously defined shape or size when subjected to appropriate thermal cycle⁽²⁾. Both Ni-Ti and copper based shape memory alloys such as Cu-Al-Ni and Cu-Zn-Al are presently available for commercial shape memory applications. Ni-Ti alloys generally have shape memory properties better than Cu based shape memory alloys but they are expensive in finished form⁽³⁾. In many applications Cu based alloys provide more economical alternative to Ni-Ti specially in thermal-mechanical actuation mechanisms⁽⁴⁾. Although early copper based shape memory alloys suffered from intergranular failure due to coarse grain structure, the recent development of fine grain Cu-based alloys has improved mechanical properties by two concept, the first is by adding alloying elements such as Ti, Zr, B and Co into Cu-Al-Zn or Cu-Al-Ni alloys during the casting, whereas the second procedure is by using powder metallurgy technique to produce these alloys⁽⁵⁾. The most of presented works by researchers had focused on the martensitic transformation mechanism in Cu-Al-Ni or Cu-Zn-Al⁽⁴⁾ and mechanical behavior of casting Cu-based alloys⁽⁶⁾. For porous Ni-Ti shape memory alloy corrosion rate is

high due to large surface area and specific surface morphology⁽⁷⁾. Stress corrosion cracking in Ni-Ti alloys had been reported by Karen, 2003⁽⁸⁾. The isothermal oxidation behavior of Ni-Ti alloy in pure oxygen over the temperature range of 450-750°C had been studied by Xu et al⁽⁹⁾, 2004. The effect of wear and services on the corrosion resistance of Ni-Ti and stainless steel stents with SEM investigation had been presented by trepanier et al⁽¹⁰⁾, 2006. Moreira et al, presented corrosion behavior of electron beam melted Ni-Ti alloy in 3.56 wt% NaCl⁽¹¹⁾. Neg et al, 2008. Studied corrosion and wear properties of laser surface modified NiTi with Mo and ZrO₂ additives⁽¹²⁾. Kumar et al, 2009 studied nanoindentation properties of Ti-Ni-Ti thin films in electrochemical sensing applications⁽¹³⁾. For Cu-Al-Ni based shape memory alloys, Abid Ali, 2007 presented investigation of preparation and mechanical characterization as well as martensitic transformation studies⁽⁵⁾. Perhaps, there is no work for sliding wear and corrosion behavior for porous Cu-Al-Ni based shape memory alloy. So that this paper aims to investigate dry sliding wear and corrosion behavior by potentiostatic studies taking in to consideration the effect of Fe additives for both wear and corrosion rate.

Experimental

The test samples are produced using powder metallurgy of Cu, Al, Ni, Fe powders, which consist of mixing, blending, compacting and sintering processes.

The table (1) shown the purity and particle size of elements

powders used in this study. The base mixture is (Cu + 13 wt% Al + 3.8 wt% Ni) prepared using ball mill for 6 hrs , other samples are prepared with (0.4 , 0.8 and 1.2 wt% Fe) . After mixing , two base samples each weighing (5,12) gram are compacting with 850 MPa using alloy tool steel mold with 14.5 mm as diameter for microstructure and potentiostatic studies , and 10 mm diameter with 20 mm high for dry sliding wear studies respectively . After compacting disk samples (4–5 mm thick and 14.5 mm diameter) were sintered at 850°C for 3 hrs. in tube furnace under argon atmosphere so as to cylindrical specimens (10 mm diameter , 20 mm high) and are allowed to cool down at the furnace cooling rate (sintered case) . Some test samples were heat treated by solution treatment at 840°C for one hour then quenched in cold water (4–7°C) (quenched state) .It's found that quenched samples in cold water have martensitic structure as in the reference⁵⁾.

Specimen preparation for microstructure examination

After sintering and quenching treatment , the samples are ground using paper grits as (180 , 400 , 800 , 1000 , 1200 , and 2000) and polished with alumina at room temperature . After this state , all samples were washed by distilled water and drying using electric drier . Light optical microscope type (Union ME-3154) with fitted digital camera is used for imaging of specimen surfaces before and after sliding wear and corrosion tests.

Sliding wear test

Dry sliding wear behavior is conducted using pin on disk concept using (860 rpm) and constant sliding distance with (14.5KN) load , the disk material is grey cast iron with 55 HRC as hardness . The sample is weighted before test using 0.0001 accuracy electric balance . After a period of time (5,10,15,20,25,30 min) , sample test is weight and weight loss during sliding wear was determined with respect to surface area . The relation between mass loss per unit area (g/cm^2) and time is drawn to calculate the wear rate for all tested specimens .

Polarization test

Corrosion behavior was conducted using the potentiostat (Mlab 200 potentiostat banch elektronike gup germany , 2008 with S1C electrochemical software calculation) in the Science and Technology Ministry , as shown in fig (1) .

The corrosion cell contains three electrode , Working , Auxiliary and Reference electrodes. The test is done in 5% NaOH solution. The corrosion surface area was (50 mm^2)

Result and Discussion

The experimental results done in this work can be categorized as follows:

Dry Sliding Wear Results

The relation between weight loss (g/cm^2) during dry sliding wear with time (min) for Cu + 13% Al + 3.8% Ni alloy before quenching case and after quenching in cold water (4–7°C) , has been shown in fig (2) . It is clear that weight loss increases with increasing time as the behavior of traditional structural

alloys. The specimen in the martensitic structure (as quenched sample) has more wear resistance than that for sintered austenitic structure . The martensite formed during quenching in Cu Al Ni has superelastic and shape memory effect so that it deforms elastically under loading. This behavior gives the sample in martensitic structure more resistance to mass loss due to friction and sliding effect. Fig (3) shows the weight loss with time relation for the base alloy in addition to the effect of Fe additives from (0.4 , 0.8 and 1.2 wt%) it is shown that increasing iron content leads to increase weight loss per unit surface area. This is probably due to oxidation effect of iron which has more affinity to interact with oxygen than any other constituent of base alloy (Cu ,Ni ,Al). Further more iron oxide is not protected , not adhered with substrate of the alloy surface , and porous . These characteristics lead to increase weight loss with increasing Fe content.

Corrosion Test Results

Fig (4) and Fig (5) show the potentiostatic curves between potential and current density for austenitic and quenched (martensitic) samples respectively. It is clear that current density for sample in austenitic structure ($633.62\mu\text{A}/\text{cm}^2$) is much greater than for martensitic structure ($336.45\mu\text{A}/\text{cm}^2$). This demonstrates that shape memory alloys have more corrosion resistance than tradition alloys due to hyper elastic behavior of polycrystalline structure. It is probable that ordering in structure caused by phase transformation is

affected on the corrosion behavior of Cu Al Ni shape memory alloys.

The effect of Fe additives on the corrosion test curves is shown in fig(6,7,and 8) for 0.4 , 0.8 and 1.2 wt% Fe respectively. It is clear that corrosion current density for (Cu + 13% Al + 3.8 Ni + 0.4 Fe) is $323.43\mu\text{A}/\text{cm}^2$ which is lower than corrosion current density for 0.8 and 1.2 wt% additives of iron which are 338.97 and $347.22\mu\text{A}/\text{cm}^2$ respectively. The iron metal is more active than Cu ,Ni and Al from the electrochemical series , the iron acts as the anode and Cu act as the cathode and when the cathodic surface area is more than that of the anodic , the corrosion rate or (corrosion current density) increases . Further more , iron oxide is not protect not adhere with the substrate and it has a porous nature so that the increasing of Fe content leads to increase of Fe ions dissolved in solution.

Microstructure Examination

Fig(9;a;b and c) shows the microstructure of the surface of alloy in the austenitic state ,dry sliding wear and after corrosion in NaOH solution .It has been clear that more plastic deformation has been occurred in the surface during sliding contact with the disk which leads to more weight loss and produces many pores or cavities on the surface as well as in the corroded state. The microstructure of the surface of alloy in the quenched state ; after dry sliding wear and after corrosion in NaOH solution shown in fig(10;a;b and c respectively).The quenched specimen loss it weight in another way. The alloy in the quenched state has superelastic behavior makes it deforms with more elastic not

permanent deformation due martensitic transformation occurred during quenching treatment⁵⁾. It is clear that martensite in Cu Al Ni shape memory alloy deforms elastically with low plastic deformation during sliding wear which leads to low pores and cavities formation. Fig (11;a;b; and c) shows the microstructure of the surface of (Cu Al Ni+0.4wt % Fe) alloy in the quenched ;after dry sliding wear and after corrosion in NaOH solution respectively . It is clear that alloy pores are oriented with the direction of sliding wear and the iron compound grains are deformed to its non adherent oxide film. The same behavior with more clarity has been shown for 0.8 and 1.2 wt% Fe in the quenched; after dry sliding wear and corrosion in NaOH solution in figs (13;a;b and c) and fig(13;a;bandc) respectively.

Conclusions

From the obtained experimental results, the following conclusions can be drawn as :

- 1- Dry sliding wear rate of Cu Al Ni shape memory alloy for sintered sample is greater than that for quenched sample .
- 2- Iron additives to Cu Al Ni lead to increase wear rate for the alloy .
- 3- Corrosion rate of austenitic Cu Al Ni is more than corrosion rate of martensitic Cu Al Ni.
- 4- Increased iron content in the base Cu Al Ni shape memory alloy from (0.4 to 1.2 wt% Fe), increases corrosion rate.

Acknowledgements

The authors would like to acknowledge the Mrs.Rehab S.Kadhim for her help in microstructure examination of tested samples at Babylon University.

References

- [1] WEZ,Z.G.,Sandstrom ,R.and Miyazaki,S., "Review Shape memory materials and hybrid composites for smart systems " ,J.Nat. Scie.33,pp.3743-3762,1998.
- [2] Noecker,R." Shape memory materials " , martensitic structures, metallography and microstructure , Vol.9,ASM Hand book , ASM international , 2004.
- [3] Wu,M.H." Cu-based Shape Memory Alloys in Engineering aspects of shape memory Alloys", edited by Duerieg ,T.and C.M.Wayman,1990.
- [4] Otsuka,K.and Ren,X." Martensitic transformation in non ferrous shape memory alloys", materials science and eng. A273-275,1999.
- [5] Abd Ali ,A.K., " Investigation of certain shape memory alloys in space systems " , PhD thesis, Babylon university , 2007.
- [6] Miyazaki, S., " Shape memory alloys " , 1999.
- [7] Itin,V., " corrosion behavior of Ti Ni based alloys in the HCl water solution " , metal protection,35,pp.373-375,1999.
- [8] Karen,Ng., " Stress corrosion cracking in Biomedical metallic implants Titanium – Nickel (Ti Ni) alloy", report for mAtE 115,Fall,2003.
- [9] Xu,C.H.,Ma,X.Q.,Shi,S.Q.and WOO,C.H., "Oxidation behavior of TiNi Shape memory alloy at 450-750 °C",Mat.Science and engg.A371,pp.45-50,2004.
- [10] Trepanier,C.,Gong,X.Y.,Ditter,T .and pelton , A., "Effect of wear and crevice on the corrosion resistance of overlapped stents " , Int.Conf.on shape memory and super elastic technologies ,may 1-11,2006.

[11] Moreira, C.T.A., Rigo, O.D., Oliveira, M.A.S., Iha, K and Ofubo, J., " Corrosion behavior of equiatomic Ni Ti SMA in solution Chloride Solution " , conf.15a, Nove.2006. Brazil.

[12] Neg, K.w., Man, H.C. and Yue, T.M., " Corrosion and wear properties of Laser surface modified seasing " , Talanta 78, pp.964-969, 2009.

Ni Ti with Mo and ZrO₂," Applied surface science 245, pp.6725-6730, 2008.

[13] Kumar, A., Singh, D., Goyal, R.N. and Kaur, D., "Fabrication and nanoindentation properties of Ti Ni/ Ni Ti thin films and their applications in electrochemical

Table (1) Shown the purity and particle size of powders used .

Powders	Purity (%)	Particle Size (µm)	Origin
Cu	99.98	68	Merck Co.
Al	99.99	80	Merck Co.
Ni	99.90	38	Merck Co.
Fe	99.80	16	Merck Co.



Figure (1) Potentio static equipment

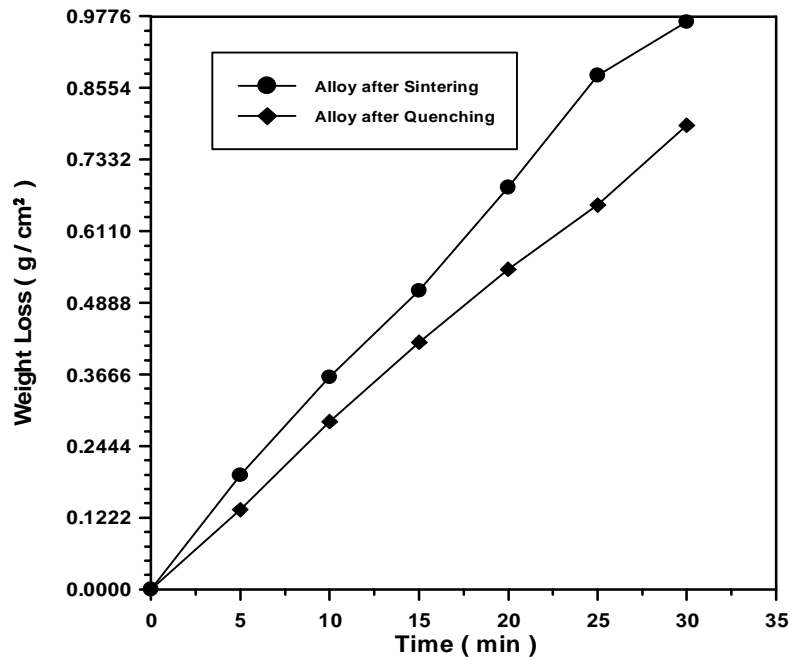


Figure (2) Shows the relation between weight loss during dry sliding with time for (Cu +13wt%Al+3.8wt%Ni) alloy in sintering case and after quenching in iced water.

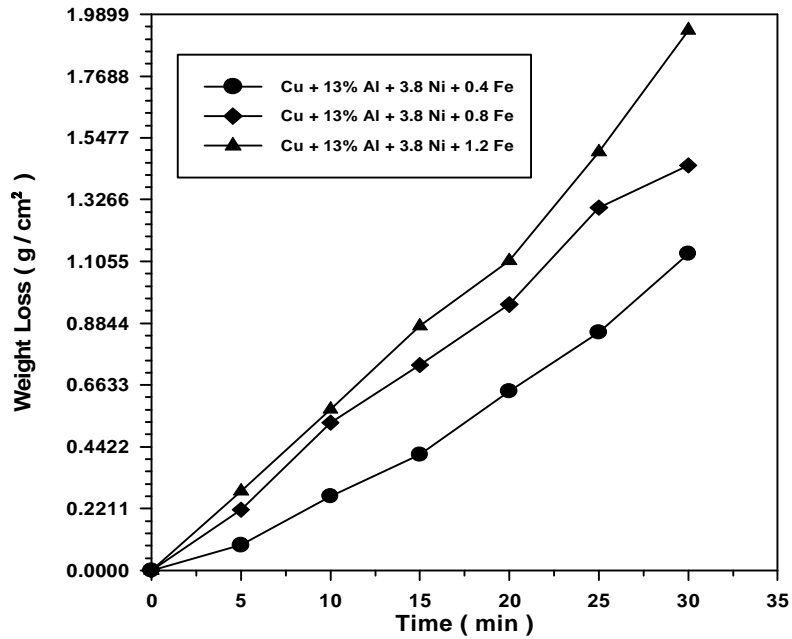


Figure (3) Shows the relation between weight loss during dry sliding with time for (Cu +13wt%Al+3.8wt%Ni) alloy with the effect of Fe additives

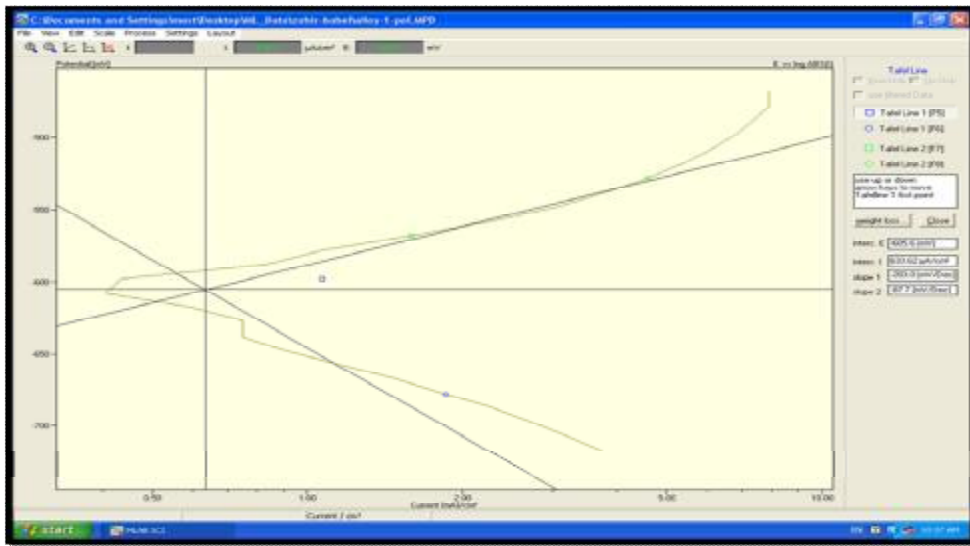


Figure (4) Show the potentiostatic curves between potential and current density for (Cu +13wt%Al+3.8wt%Ni) alloy in sintering case.

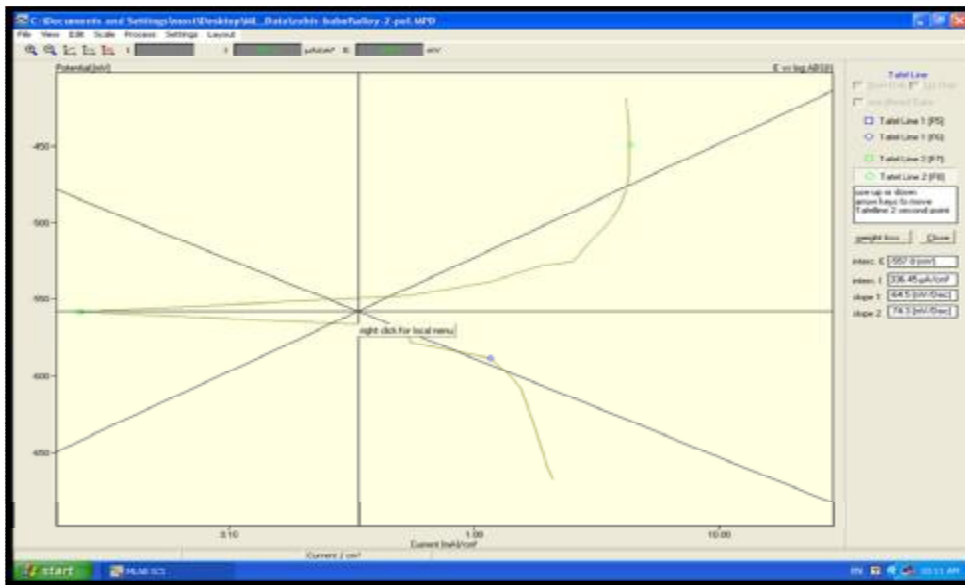


Figure (5) Show the potentiostatic curves between potential and current density for (Cu +13wt%Al+3.8wt%Ni) alloy after quenching in cold water.

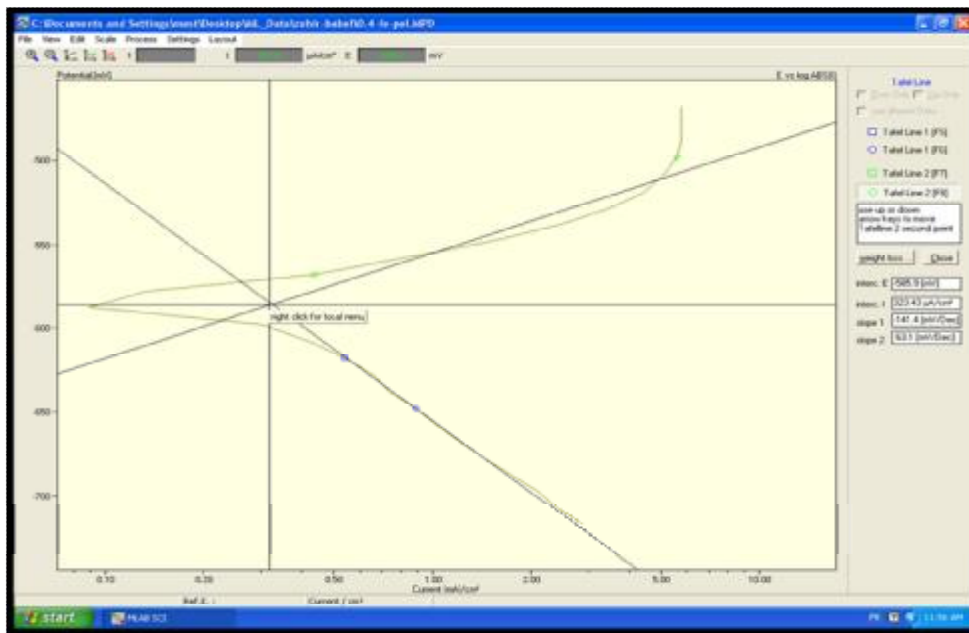


Figure (6) Show) Show the potentiostatic curves between potential and current density for (Cu +13wt%Al+3.8wt%Ni + 0.4wt% Fe) alloy.

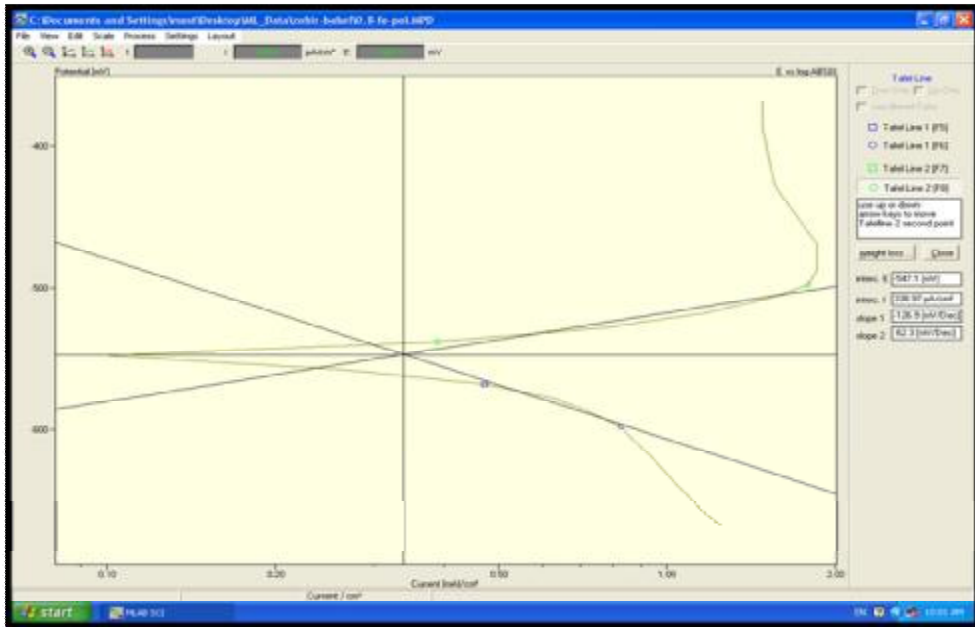


Figure (7) Show the potentiostatic curves between potential and current density for (Cu +13wt%Al+3.8wt%Ni + 0.8wt% Fe) alloy.

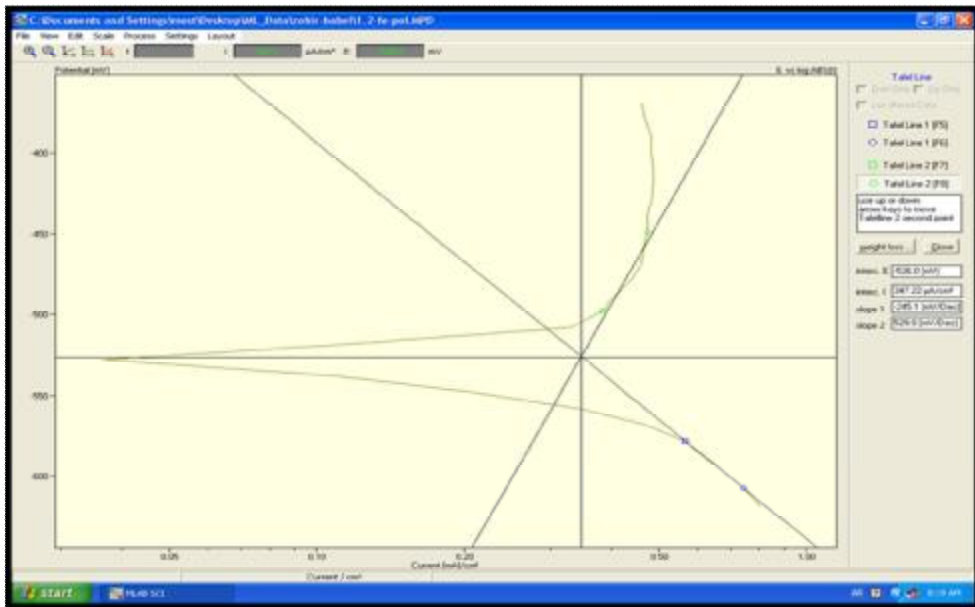
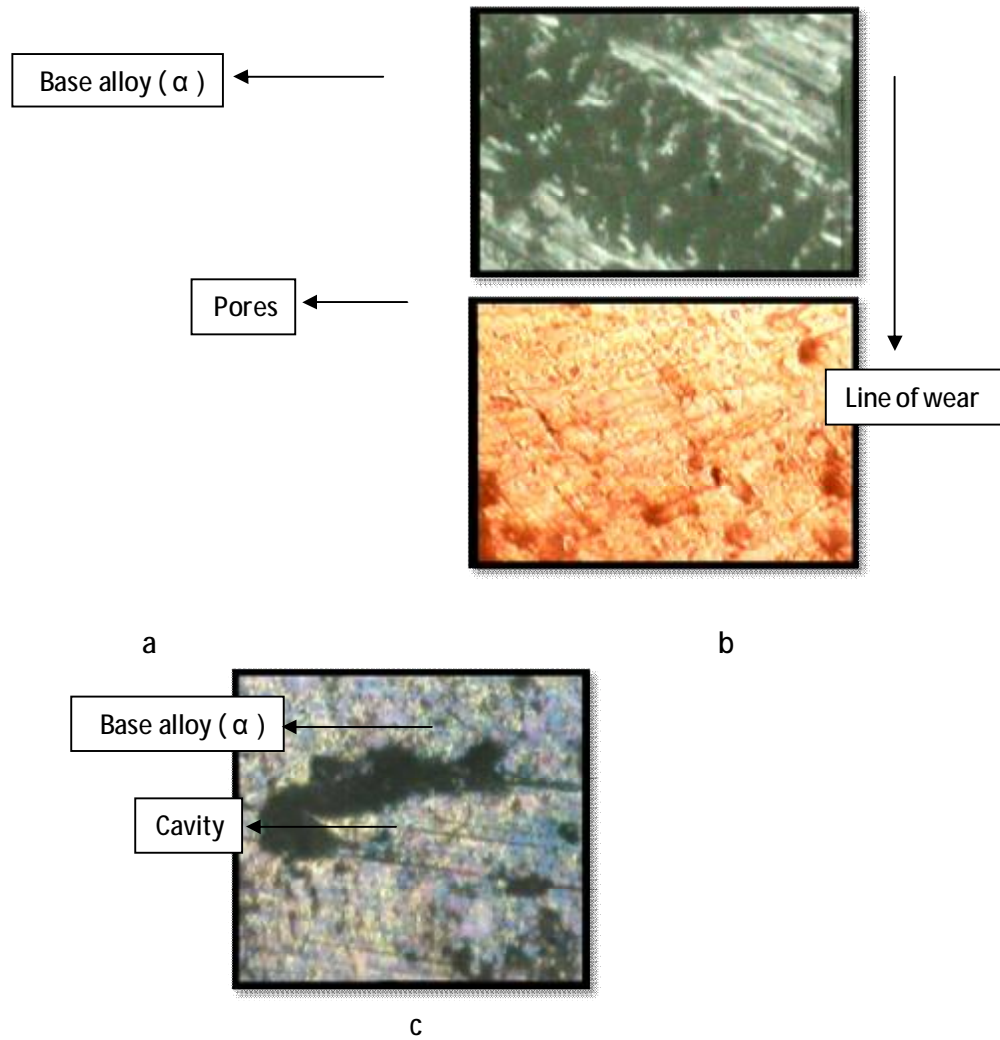


Figure (8) Show the potentiostatic curves between potential and current density for (Cu +13wt%Al+3.8wt%Ni + 1.2wt% Fe) alloy.



**Figure (9) a-Surface alloy in sintered case(750X).
b-Surface of alloy in sintering case after dry sliding wear (750X).
c-Surface of alloy in sintered case after corrosion test (750X).**

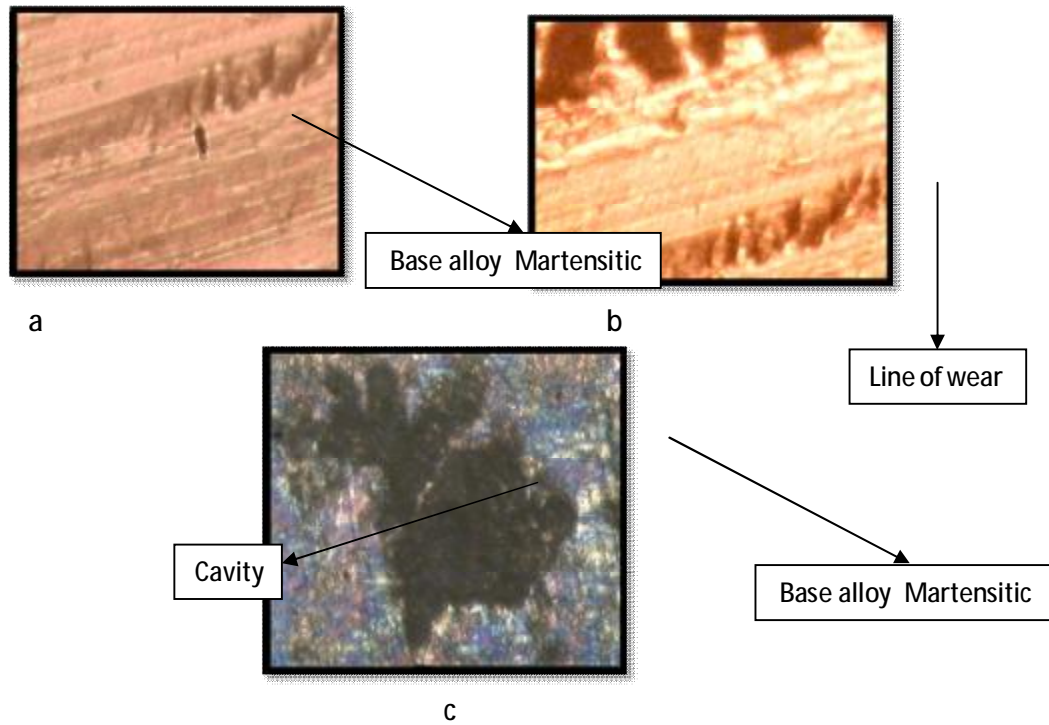


Figure (10)a- Surface of alloy after Quenching in iced water (750X).
b-Surface of alloy in quenching case after dry sliding wear (750X).
c- Surface of alloy in quenching case after corrosion test (750X).

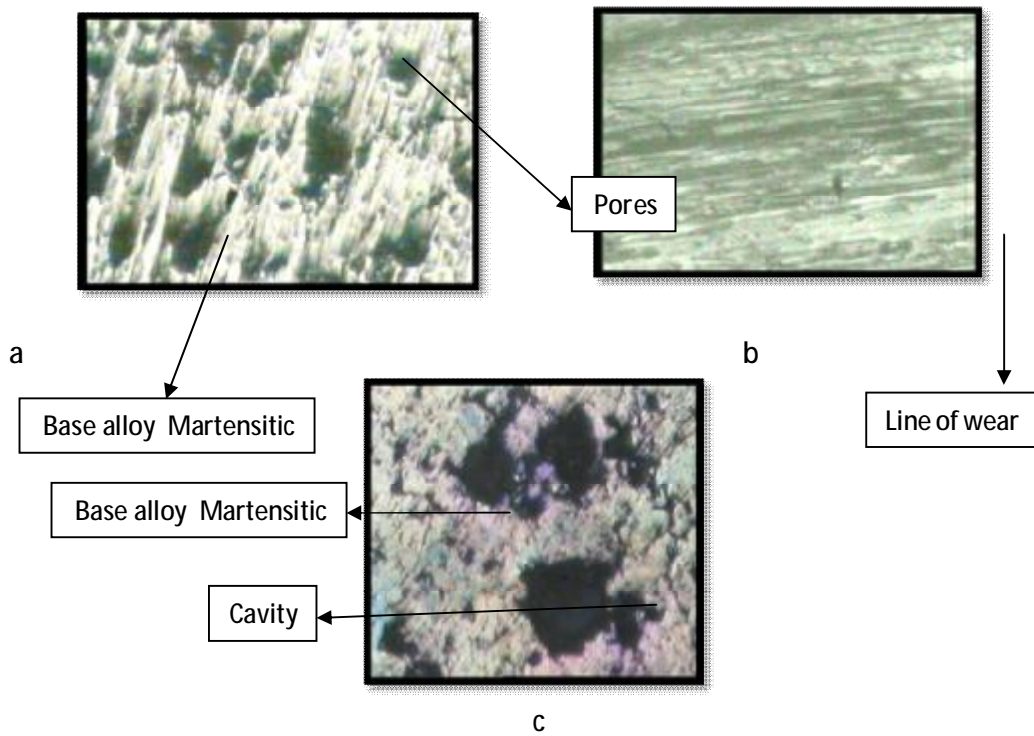


Figure (11) a- Surface of (Cu +13wt%Al+3.8wt%Ni+0.4wt% Fe) alloy (750X) as quenched condition .

b-Surface of (Cu +13wt%Al+3.8wt%Ni+0.4wt% Fe) alloy after dry sliding wear (750X).

c-Surface of (Cu +13wt%Al+3.8wt%Ni+0.4wt% Fe) alloy after corrosion test (750X).

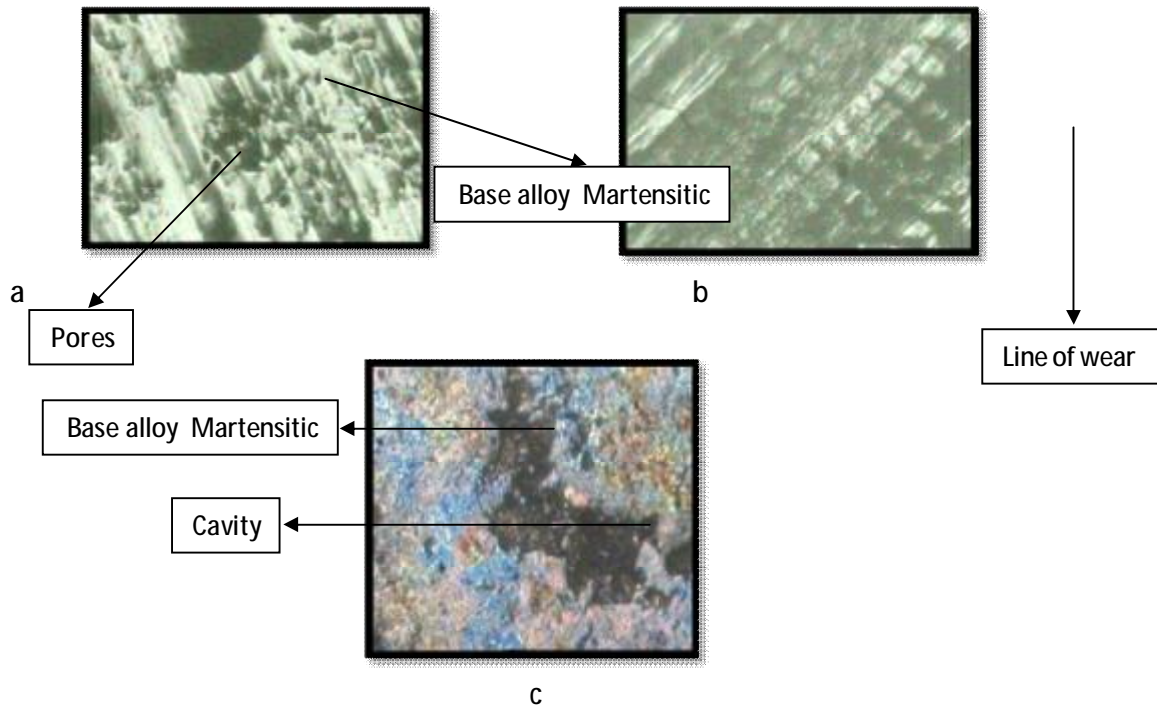


Figure (12) a-Surface of (Cu +13wt%Al+3.8wt%Ni+0.8wt% Fe) alloy (750X) as quenched condition.
B-Surface of (Cu +13wt%Al+3.8wt%Ni+0.8wt% Fe) alloy After dry sliding wear (750X).
C-Surface of (Cu +13wt%Al+3.8wt%Ni+0.8wt% Fe) alloy After corrosion test (750X).

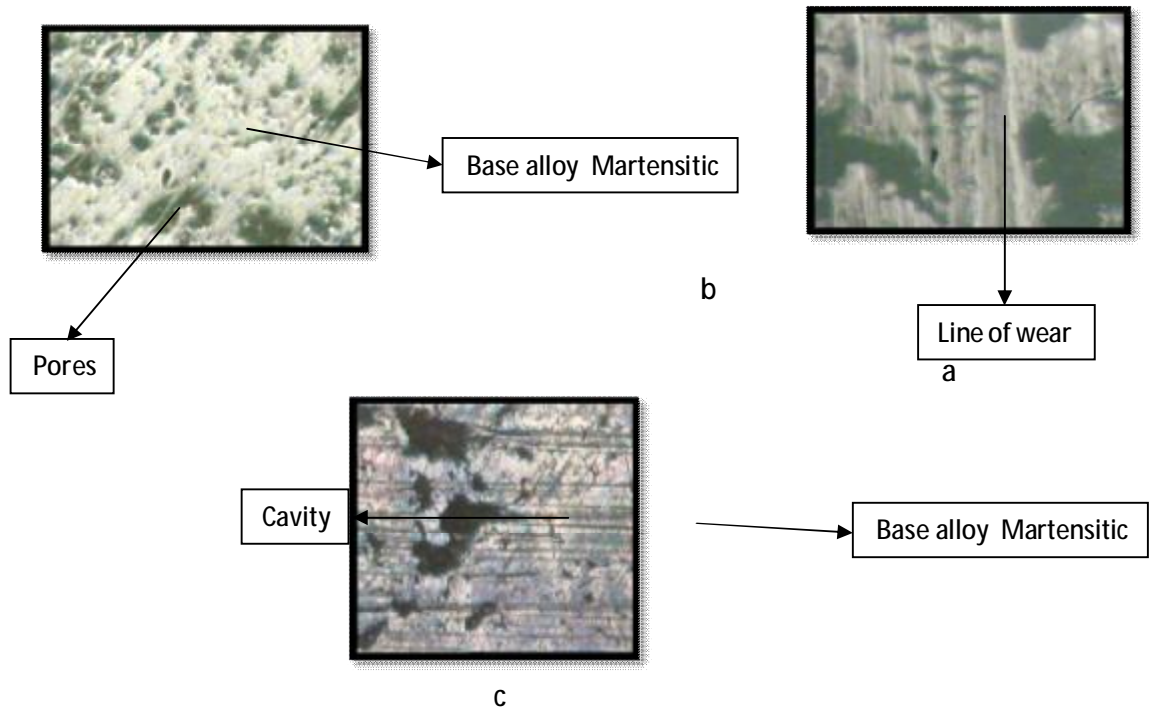


Figure (13)a- Surface of (Cu +13wt%Al+3.8wt%Ni+1.2wt% Fe) alloy (750X) as quenched condition.

b-Surface of (Cu +13wt%Al+3.8wt%Ni+1.2wt% Fe) alloy after dry sliding wear (750X).

c-Surface of (Cu +13wt%Al+3.8wt%Ni+1.2wt% Fe) alloy after corrosion test (750X).